23rd Australasian Fluid Mechanics Conference - 23AFMC
Sydney, Australia
4 – 8 December 2022
Paper No: AFMC2022-100

Development and validation of digital twin to design wing attitude controller

Morgan van Hoffen[1*] **and Ingo H. J. Jahn**[2]

[1] University of Southern Queensland, Springfield, QLD 4300, Australia
*Email: morgan.vanhoffen@usq.edu.au

Abstract

There is renewed interest in high-speed flight for commercial and defence applications. To achieve desired performance for stability and manoeuvrability these vehicles require highly effective control systems, mechanical actuators, and robust control strategies. The challenge of aircraft control law derivation has seen extensive research, however simulation-based approaches lack validation testing on real flight hardware and full-scale flight tests only take place late in the development process when design changes are prohibitively expensive. A coupled approach using both ground testing of sub-scale models and a Digital Twin of the dynamic and embedded system offers efficient control system design and valuable insight into practical flight control performance at the early stages of the development process. This paper presents the methodology employed to determine aerodynamic and dynamic characteristics for a subsonic wind tunnel model and the corresponding control-oriented modelling to generate the Digital Twin. To demonstrate the approach, a proportional-integral-derivative (PID) feedback controller was developed using the Digital Twin and corresponding gain settings were applied to the experimental model. Using a test case involving step changes in wing angle-of-attack it was shown that both systems responded consistently and the significant dynamic effects were captured accurately in the Digital Twin system representation.

1 Introduction

The design and testing of flight control systems are inherently multi-faceted, and for supersonic and hypersonic speeds can be particularly challenging due to the coupling of aerodynamic, thermal and propulsive requirements (Bowcutt 2018). Furthermore, these vehicles often require expensive full-scale flight tests for validation, a process which can often only be performed late in the design stage (McNamara 2011). Digital Twin system representations (hardware-in-the-loop simulations) have been used widely to model and predict the dynamic response of real systems for aircraft and automotive applications, however dynamic force predictions are often derived from numerically simulated estimates (Bacic 2012). Whilst computational methods provide valuable insight for control and stability margins, instances such as the failure of the flight flight test of the NASA X-43A in 2001, highlight the importance of accurately capturing all vehicle dynamic characteristics for vehicle flight stability analysis (Hughes 2002). Several other flight vehicle failures are attributed to modelling inaccuracies including the DARPA sponsored HyCAUSE scramjet program (Walker 2008) and the NASA X-51A in 2010 and 2011 (Lewis 2010).

Evidently, when designing flight control systems, there is a need to consider aerodynamic characteristics which include the contributions and interactions of real flight conditions, not just those which are simulated. One approach is using a Digital Twin with experimentally measured aerodynamics to develop and tune a system, followed by hardware-in-the-loop ground tests. With this goal in mind, to overcome the high operating costs and test time limitations of hypersonic test facilities, continuous running subsonic facilities can be used to develop the methodology. With the approach confirmed it can be adapted to suit short duration tests in hypersonic facilities. The paper presents the development of a Digital Twin of a subsonic wind tunnel model using experimentally measured wing pitching moments for a range of angle-of-attack and trailing edge flap angles. This approach was previously used

by Bacic (2012) to implement a feedback controller to drive the experimental and simulated system to a desired angular setpoint and compare dynamic response. The aim of this work is to show that tuning the controller in the Digital Twin results in the same dynamic response as tuning the controller on the experimental model. With validation of the method for singular flow velocity, the platform will allow for development of more advanced control laws.

This paper is structured as follows: Section 2 describes the experimental hardware, corresponding physical characteristics and the methods for determination of the model aerodynamics, Section 3 introduces the Digital Twin simulation structure, Section 4 presents the closed-loop control test case and discusses the results, and finally, Section 5 concludes the paper.

2 Subsonic Experimental Model

The subsonic experimental model discussed in this paper acts as a physical platform to conduct research and validate the development of a Digital Twin. The model has two key purposes. First, it allows for generation of an aerodynamic database to be included in the Digital Twin, and second, it can be used to test the hardware implementation for the embedded control system and the performance of control methods. This section introduces the physical hardware and the methodology to determine the aerodynamics.

2.1 Model Description

The model hardware used in this campaign was experimentally tested in the University of Queensland Aerolab subsonic wind tunnel. For this campaign a motor speed of 1000 RPM was selected, corresponding to a flow velocity of 26.8 m/s. The model properties are provided in Table 1.

The model used for this campaign consists of a NACA0018 symmetric wing profile with an actuated trailing edge flap, mounted on a rotating support shaft at the quarter chord (see Figure 1). The model is 168mm long and 300mm wide, with a trailing edge flap length of 58mm and width of 100mm. This symmetric wing profile was selected with the purpose of providing consistent aerodynamic forcing for positive and negative angles of attack and the trailing edge flap length was selected experimentally to ensure control authority across the operational regime. The actuation of the trailing edge flap is controlled by a 13mm brushless motor mounted internally forward of the support shaft and connected via push-pull rods. In the effort to ensure the flow remains largely 2-dimensional over the actuated section of the wing elliptical sections were added to side of the centre section as shown in Figure 1.

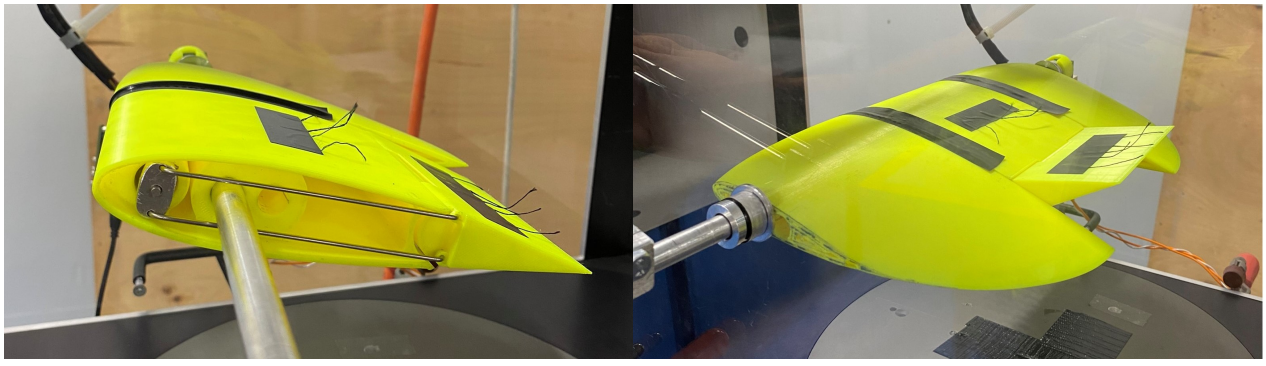

Figure 1. Model with one elliptical section removed and the internal mechanism exposed (left) and assembled model mounted with deflected trailing edge flap (right).

The wing is free to rotate in the tunnel. During the test the trailing edge flap is deflected by an angle (β) to control the wing angle-of-attack (α). The angle-of-attack is provided to the controller

from an angular position sensor mounted external to the wind tunnel on the hollow support shaft which supports the model in the flow. This aluminium shaft also provides passage for the flap actuator signal and power wiring.

Table 1. Experimental model physical parameters.

Parameter	Description	Value	Units
V	Flow velocity	26.8	m/s
ρ	Flow density	1.225	kg/m^3
S	Wing planform area	0.041	m^2
c	Chord length	0.168	m
I_w	Wing moment of inertia	7.27×10^{-4}	kgm^2
m	Mass of calibration weight	-	kg
x	Calibration arm length	0.1	m
m_{model}	Mass of model	0.35	kg
x_{model}	CoG location of model	0.0186	m
m_a	Calibration arm mass	0.0162	kg
x_a	Calibration arm CoG distance	0.045	m

2.2 Embedded System Hardware

The embedded system hardware for the subsonic model includes a Raspberry Pi 3b, AMS AS5145 magnetic position encoder and a Maxon ECXSP13M brushless motor. The motor features a 125:1 planetary gearhead with a built-in position encoder providing a resolution of 1024 counts per revolution. The EPOS studio software allowed the internal position control loop to be tuned and saved to the motor driver board. The closed-loop control software was written in Python on the Raspberry Pi and provides a position command to the EPOS motor driver. Due to a lack of software interrupts between the control loops, in the current implementation, the outer loop ran at a frequency of 6.5Hz. The block diagram for the physical hardware is shown in Figure 2. This includes the position control loop with angular feedback from the encoder on the support shaft, and the inner control loop of the EPOS driver board.

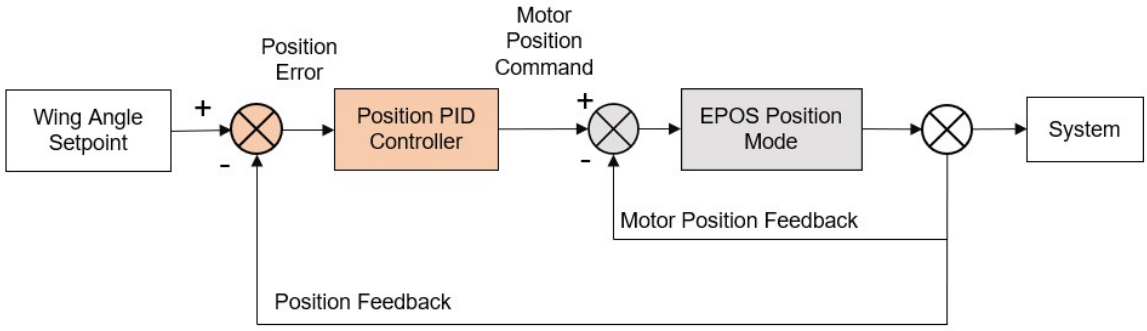

Figure 2. Experimental wing angle controller stabilising on angle setpoint including the inner-loop managed by the EPOS motor driver to provide accurate positioning control.

2.3 Model Aerodynamic Characterisation

The determination of aerodynamic pitching moment was performed by changing the mass hanging from a calibration arm mounted to the support shaft of the model. These masses indicate the moment required to create equilibrium between the applied load and the aerodynamic forcing of different flap

and wing angles and hence represent the static contribution to the total pitching moment. Figure 3 illustrates the free-body diagram of the experimental configuration including contributions from the hanging mass, calibration arm mass and moment of the model due to gravity.

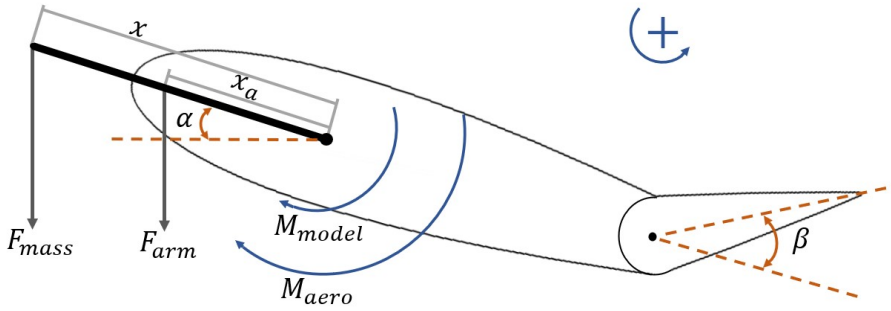

Figure 3. Free-body diagram of testing apparatus for measurement of wing pitching moments at varying angles of attack.

Summation of the moments on the body around the rotational axis allows for determination of the aerodynamic pitching moment.

$$M_{aero} = M_{mass} + M_{arm} - M_{model} \tag{1}$$

Substituting known lengths and masses provides:

$$M_{aero} = m\,g\,x\cos\alpha + m_a\,g\,x_a\cos\alpha - m_{model}\,g\,x_{model}\cos\alpha \tag{2}$$

The wing aerodynamic characteristics can be approximated using a polynomial curve-fit, created with the Curve Fitting Tool in MATLAB. Experimental results and the curve-fit are presented in Figure 4. The curve is third degree in wing angle and first degree in flap angle. This allows for easier root-finding when calculating the initial flap angle. The fit has an R squared value of 0.97 and RMSE of 0.0134. The curve fit takes the form:

$$M_{aero} = p_{00} + p_{10}\alpha + p_{01}\beta + p_{20}\alpha^2 + p_{11}\alpha\beta + p_{30}\alpha^3 + p_{21}\alpha^2\beta \tag{3}$$

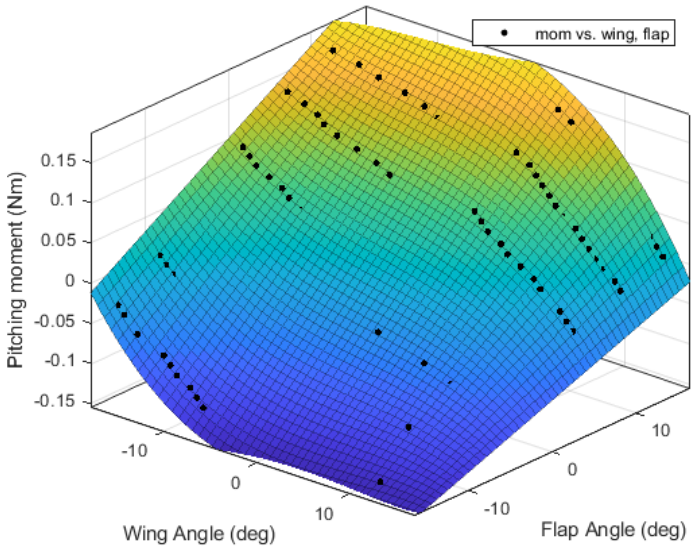

Figure 4. Subsonic model aerodynamic pitching moment for varying angle-of-attack and flap angles. Moment resolved around pitching axis of model.

The aerodynamics model provides insight into the control authority of the trailing edge flap for varying angle-of-attack. Notably for the maximal case of $\pm 15^\circ$ angle-of-attack there remains a small restoring pitching moment when the full flap deflection of $\pm 15^\circ$ is applied. This represents the most extreme case where the control surface is deflected behind the body and likely experiencing partial flow separation. Evidently, the system has dynamic stability and control authority at the extremes of the test regime. Additionally, an inflection point in the system aerodynamics was noted at 0° angle-of-attack. This was attributed to the shifting forward of the aerodynamic centre-of-pressure beyond the pitching axis resulting in static instability.

3 Digital Twin Model

The Digital Twin hardware-in-the-loop simulation aims to recreate the dynamic response of the physical hardware by time-stepping the pitching motion. It includes contributions from the experimental aerodynamics model presented in Section 2.3 and damping due to friction of the system. This section introduces the dynamic equations and the structure of the simulation.

3.1 Aerodynamic Simplifications

The pitching moment of the wing is known to be a function of angle-of-attack, flap angle, and respective rates. As a leading order approximation, the moment can be defined as:

$$M_{aero} = M(\alpha, \dot{\alpha}, \beta, \dot{\beta}) \tag{4}$$

Additionally, the pitching motion can be separated into static and dynamic contributions.

$$M_{aero} = M_{static}(\alpha, \beta) + M_{dynamic}(\alpha, \dot{\alpha}, \beta, \dot{\beta}) \tag{5}$$

For cases where $\dot{\alpha}$ and $\dot{\beta}$ are small the dynamic contribution can safely be excluded. However, whilst the wing is in motion this will not be a valid assumption and higher model mismatch will exist between the experimental and simulated systems. In the Digital Twin only static or steady-state aerodynamic moments are considered as per Section 2.3. That is:

$$M_{aero} = M_{static}(\alpha, \beta)$$

3.2 Dynamics Model

The Digital Twin model takes the standard form of a non-linear dynamic system where the change in system state for each time step of the simulation is given as:

$$\dot{x} = \mathbf{f}(x, u) \tag{6}$$

Where,

$$x = [\alpha, \dot{\alpha}]^T, \qquad u = [\beta]$$

The simulation approach, illustrated in Figure 5, uses the well established Runga-Kutta 4th order integration method loop to time-step the system dynamics. By definition of the system initial conditions,

$$x_0 = \begin{bmatrix} \alpha_0 \\ \dot{\alpha}_0 \end{bmatrix}$$

the dynamic response can be characterised by the following equations, where $M_{aero}(\alpha, \beta)$ is the experimental model outlined in Section 2.3, I_w is the wing moment of inertia and c is the damping

coefficient.

$$\dot{x} = \begin{bmatrix} \dot{\alpha} \\ \ddot{\alpha} \end{bmatrix} = \begin{bmatrix} \dot{\alpha} \\ (\mathbf{M}_{aero}(\alpha, \beta) - c\dot{\alpha})/I_w \end{bmatrix} \tag{7}$$

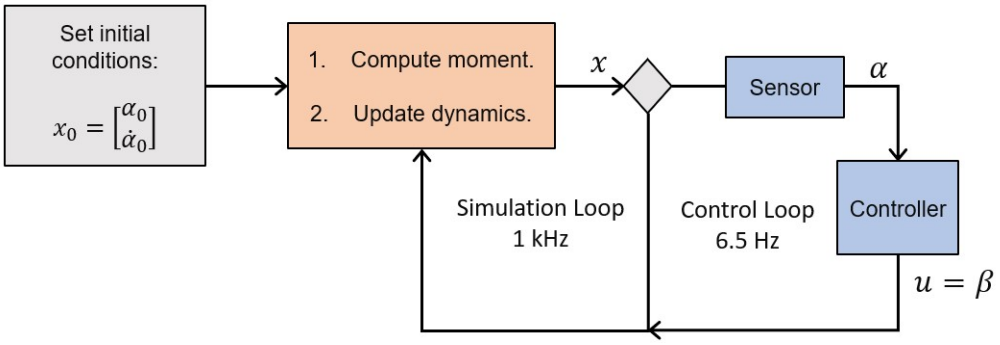

Figure 5. Simulation loop for subsonic pitching dynamics.

The simulation uses a proportional-integral-derivative (PID) controller to drive the system towards a target angle-of-attack. The controller uses angle-of-attack α measured by the shaft encoder as an input, and flap angle β as the control output. This formulation is presented in Section 4 however specific characteristics were included in the Digital Twin representation to ensure accuracy. Firstly, the update frequency of the control loop of the physical system was limited due to the lack of software interrupts between the embedded system and the actuator. Consequently, the physical system only performed closed-loop control at a rate of 6.5Hz, whilst the main simulation loop was updated at 1kHz. The damping coefficient of the system was estimated to be $c = 9 \times 10^{-3}$ by comparing the number of oscillations and peak overshoot of the simulated and experimental systems.

4 Closed-loop Control Validation

To verify the Digital Twin system approach, simulations are compared to experimental tests, both using the same feedback controller. This approach allows comparison of the response of the experimental and simulated systems to ensure that significant dynamic characteristics are accurately modelled. Furthermore, this test-case provides an opportunity to assess the performance of the experimental hardware for position control.

4.1 PID Control

The experimental and simulated systems are configured with a PID controller which calculates an error value $e(t)$ as the difference between the desired setpoint (SP) and a measured process variable (PV). The controller sums the contribution of each term and applies a correction based on proportional K_p, integral K_I, and derivative K_D gains. The controller output U is calculated from the following control function:

$$U(t) = K_p e(t) + K_i \int_0^t e(t)dt + K_D \frac{de(t)}{dt} \tag{8}$$

This was implemented in the code where the SP was specified by the user and the PV was measured by the angular position encoder for wing angle-of-attack. As a result the units are degrees and the output of the PID controller is a scaled angular position command for the motor.

4.2 Closed-loop Test Case

Presented is a closed-loop test to drive the wing angle-of-attack from 2° to 16°. The system initial state is:

$$x_0 = [\alpha, \dot{\alpha}]^T = [2, 0]^T$$

The experimental initial flap angle is chosen when equilibrium occurs at the desired starting angle-of-attack. The simulation initial flap angle is calculated from the aerodynamics model by setting the total moment to zero and solving for flap angle at the desired initial angle-of-attack. Due to model mismatch initial flap angles vary for the simulated and experimental tests.

$$u_{0,Sim} = -1.36^\circ, \qquad u_{0,Exp} = -8.98^\circ$$

For both systems the control loop is run at 6.5Hz to reflect the physical hardware performance. Furthermore, due to a delay in the start-up process between the EPOS driver board and the embedded controller an initial delay of 1s is added to the simulation to reflect the integral wind-up which takes place on the physical hardware. Figure 6 shows the response of the system for the test case. Both datasets are plotted at 6.5Hz, corresponding to the control update rate and sampling rate from the experiment. In addition the simulation is plotted at 100Hz to show transients not captured by the low sampling frequency. Controller gains were tuned using the well-established Zieger-Nichols heuristic tuning method. In this case a PI controller was deemed suitable and the following gains were applied to the experimental and simulated systems:

$$K_p = 0.3, \qquad K_I = 0.8, \qquad K_D = 0.0$$

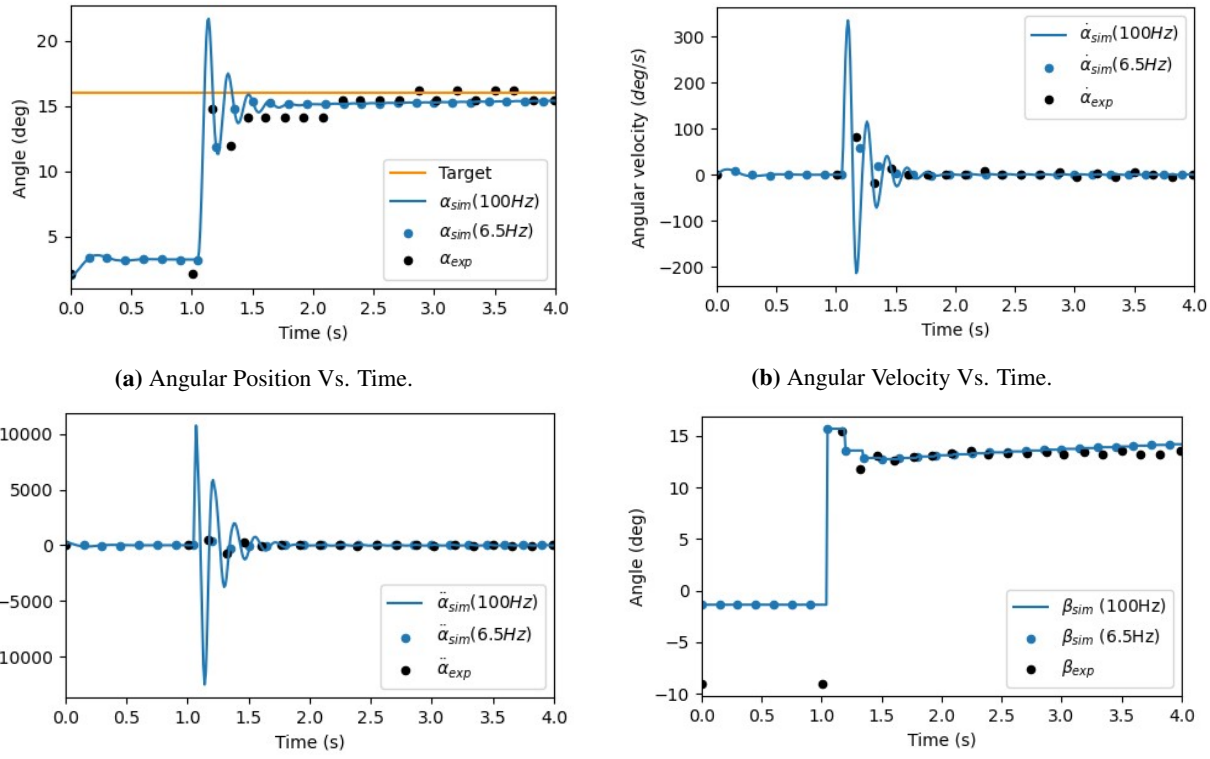

(a) Angular Position Vs. Time.

(b) Angular Velocity Vs. Time.

(c) Angular Acceleration Vs. Time.

(d) Flap Angle Vs. Time.

Figure 6. Closed-loop test case with setpoint for wing angle-of-attack of 16°.

4.3 Discussion

The results illustrate that the Digital Twin representation is able to closely recreate the dynamic behaviour of the real system when corresponding controller gains are applied and the control system

is operated at the same rate. This is shown in Figure 6a and 6d, where both systems reach the setpoint of 16° and equilibrium flap position of 14° at approximately 2 seconds. The peak angular velocity and accelerations experienced by each system are highly dependent on sampling frequency. This is shown in Figure 6b and 6c, where there is good correlation when plot at 6.5Hz. However, plotting at 100Hz shows high frequency dynamics not resolved by the low sample rate resulting in aliasing of the data. The experimental results presented in Figure 6 demonstrate the ability of the experimental system to track the desired setpoint despite hardware limitations of the controller and an angular position resolution of the magnetic encoder of 0.7°.

Some model mismatch can be noted at the initial angle-of-attack of 2° where there is a large difference in equilibrium flap position between the experimental and simulated system. This can be attributed to the reduced order curve fit and difficulty to collect experimental data around the inflection point at 0°. In contrast, good agreement between the hardware and Digital Twin is observed at higher angles-of-attack as shown by the correlating final control output of approximately 14° at the desired setpoint. The results indicate that the simplified steady aerodynamics model is suitable to apply for angular position control in the largely linear regions of the aerodynamic map, and controller gains which are tuned in simulation can be applied and work successfully in reality.

The subsonic wind tunnel model discussed in this paper acts as a stepping-stone towards the goal of hypersonic closed-loop wind tunnel testing. The lessons learnt herein show the value of capturing real system aerodynamics and that the approach of tuning control systems using a Digital Twin is valid. Future work will aim to improve the modelling methods and reduce model mismatch by coupling inviscid, steady computational-fluid-dynamic simulations with experimentally measured pitching rates. The Digital Twin will then be used to apply gain scheduling methods to tune the controller for multiple linear regions and produce improved tracking performance. Furthermore, the subsonic hardware highlights the importance of embedded systems which allow motor commands and data collection to operate at frequencies which accurately capture system dynamics. This will be vital for future hypersonic wind tunnel testing where flow timescales are fractions of a second and system dynamics are required to be significantly faster.

5 Conclusions

This paper presents the method to design a Digital Twin system representation for a subsonic wind tunnel model based on experimentally derived aerodynamic data, and evaluates the model with a closed-loop test case. The results presented show that despite limitations in the physical hardware, the Digital Twin captures the significant dynamic effects and can be used as a cost effective and efficient tool for controller development and tuning for aerodynamic systems.

Acknowledgements

Morgan van Hoffen is supported by an Australian Government Research Training Scholarship.

References

Bowcutt, K., 2018, *Physics Drivers of Hypersonic Vehicle Design*, 22nd AIAA International Space Planes and Hypersonics Systems and Technologies Conference.

McNamara, J., Friedmann, P., 2011, *Aeroelastic and Aerothermoelastic Analysis in Hypersonic Flow: Past, Present, and Future*, AIAA: Volume 49, Number 6.

Bacic, M., MacDiarmid, M., 2012, *Hardware-in-the-loop Simulation of Aerodynamic Objects*, AIAA Modeling and Simulation Technologies Conference and Exhibit.

Hughes, R. (chairman), 2002, *Report of findings X-43A Mishap*, Mishap Investigation Board.

Walker. S., Frederick. R., Paull. A., van Wie. D., 2008, *HyCAUSE Flight Test Program*, 15th AIAA International Space Planes and Hypersonic Systems and Technologies Conference.

Lewis. M., 2010, *X-51 scrams into the future*, Aerospace America: Volume 48, Pages 26-31.